A Graph Automorphic Approach for Placement and Sizing of Charging Stations in EV Network Considering Traffic

Hossein Parastvand, *Student Member, IEEE*, Valeh Moghaddam, *Member, IEEE*, Octavian Bass, *Senior Member, IEEE*, Mohammad A. S. Masoum, *Senior Member, IEEE*, Airlie Chapman, *Member, IEEE*, and Stefan Lachowicz, *Senior Member, IEEE*

***Abstract*—This paper proposes a novel graph-based approach with automorphic grouping for the modelling, synthesis, and analysis of electric vehicle (EV) networks with charging stations (CSs) that considers the impacts of traffic. The EV charge demands are modeled by a graph where nodes are positioned at potential locations for CSs, and edges represent traffic flow between the nodes. A synchronization protocol is assumed for the network where the system states correspond to the waiting time at each node. These models are then utilized for the placement and sizing of CSs in order to limit vehicle waiting times at all stations below a desirable threshold level. The main idea is to reformulate the CS placement and sizing problems in a control framework. Moreover, a strategy for the deployment of portable charging stations (PCSs) in selected areas is introduced to further improve the quality of solutions by reducing the overshooting of waiting times during peak traffic hours. Further, the inherent symmetry of the graph, described by graph automorphisms, are leveraged to investigate the number and positions of CSs. Detailed simulations are performed for the EV network of Perth Metropolitan in Western Australia to verify the effectiveness of the proposed approach.**

***Index Terms*—Electric vehicle, portable charging station, placement, sizing, fast charging, controllability.**

NOMENCLATURE

Abbreviations

PBH	Popov-Belevitch-Hautus.
CEA	Community energy association.
CN	Complex network.
CS	Charging station.
ECM	Exact controllability method.
EV	Electric vehicle.
LQR	Linear quadratic regulator.
PCS	Portable charging station.
PEV	Plug-in electric vehicle.

Constants

ε	Identity (or trivial) permutation.
c	A complex number.
Q, R, Y	Arbitrary weights.

Parameters

δ_i	Maximum algebraic multiplicity of $\lambda_(i)$.
λ^M	Maximum algebraic multiplicity of teh eigenvalue λ^M.
λ_i	The i^{th} eigenvalue.
ν	A point (node) of permutation.
σ	Permutation.
$\mathcal{A}$	Adjacency matrix.
$\mathcal{G}$	Graph.
$\mathcal{K}$	Optimal feedback gain vector.
$\mathcal{L}$	Laplacian matrix.
$\mathcal{S}$	Determining set.
$\mathrm{Aut}(\mathcal{G})$	Automorphism group.
$\mathrm{dim}V_{\lambda_i}$	Dimension of eigenspace associated with $\lambda(i)$.
$\mathrm{Fix}(\sigma)$	The set of fixed nodes by permutation.
$\mathrm{Gen}(\mathcal{G})$	Generators of automorphism.
$\mathrm{Move}(\sigma)$	The set of moved nodes by permutation.
$\mu(\lambda_i)$	Maximum geometric multiplicity of $\lambda(i)$.
A	State matrix.
a_{ij}	Weight of ij^{th} element of $\mathcal{A}$.
B	Input matrix.
C	Size (or capacity) of charging station [kW].
E	The set of edges.
m	Index of a permutation.
N_D	Number of required driver nodes.
P	The solution of Riccati equation.
T	Waiting time [min].
u	Control signal (charging supply).
V	The set of nodes.
$\lvert\cdot\rvert$	Cardinality (size) of a set.

Manuscript received September 11, 2019; revised January 15, 2020 and February 26, 2020; accepted March 11, 2020. Date of publication April 3, 2020; date of current version August 21, 2020. This work was supported by Open Access Funding Support Scheme of Edith Cowan University. Paper no. TSG-01342-2019. *(Corresponding author: Hossein Parastvand.)*

Hossein Parastvand, Octavian Bass, and Stefan Lachowicz are with the Smart Energy Systems Research Group, School of Engineering, Edith Cowan University, Joondalup, WA 6027, Australia (e-mail: h.parastvand@ecu.edu.au; o.bass@ecu.edu.au; s.lachowicz@ecu.edu.au).

Valeh Moghaddam is with the School of Information Technology, Deakin University, Geelong, VIC 3220, Australia (e-mail: valeh.moghaddam@deakin.edu.au).

Mohammad A. S. Masoum is with the Department of Engineering, Utah Valley University, Orem, UT 84058 USA (e-mail: m.masoum@ieee.org).

Airlie Chapman is with the Department of Mechanical Engineering, School of Engineering, University of Melbourne, Melbourne, VIC 3010, Australia (e-mail: airlie.chapman@unimelb.edu.au).

Color versions of one or more of the figures in this article are available online at http://ieeexplore.ieee.org.

Digital Object Identifier 10.1109/TSG.2020.2984037

I. Introduction

ELECTRIC vehicles (EVs) powered by electricity from low carbon emission grids can provide significant benefits by reducing transportation impact on climate and grid's reliance on oil-based fuels. EVs provide a quiet and cleaner environment while reducing the operation and maintenance costs [1]. Plug-in electric vehicles (PEVs) which are an integration of battery and plug-in hybrid electric vehicles are key innovations to attain low-carbon transportation [2].

As the expectations for future EV sales increase, there is a growing number of researches focusing on the development of charging infrastructure indicating their importance in the early stage of EV market [3]. According to community energy association (CEA), the charging infrastructure is broadly divided into three categories based on the EV charging speeds. The standard levels of PEVs charging are AC level 1, AC level 2 and DC Charging. The AC level 1 typically takes 10-20 hours to charge [4], [5]. The long charging time makes Level 1 chargers mostly suitable for home usage. The AC Level 2 typically takes 4-5 hours to charge and can be used for both commercial and home charging. The DC charging (also called fast charging) is the fastest option and can achieve full charge in 10 to 15 minutes [4], [5]. Additionally, portable charging stations (PCSs) have recently emerged as an alternative for charging stations to deliver extra capacity during peak hours or in emergency occasions [6]. Unlike fixed stations, PCSs do not impose much construction and maintenance cost, and are not constrained with power grid capacity or the size of the site based on control [7]. The trunks equipped with battery storage feature either the lightweight lithium battery or the electric double-layer capacitor technologies [8], [9]. Both technologies can supply all charging levels. Throughout this paper, fast charging is assumed at all EV charging stations (CSs).

To increase the uptake rate of EVs, governments and automotive industries in most developed countries have been working together, and have undertaken projects to deploy a network of electric CSs, commonly known as EV networks [10]. EV networks are anticipated to play a critical role in coming decades as the forecast for PEV market growth looks very promising [11]. This is mainly due to increasing supports from governments and automotive industries.

The bulk of EV charging demand is synchronized with daily driving patterns. The anticipated challenges associated with the increasing number of EVs are long waiting times at public CSs with impacts on actual road traffic patterns and the electricity demand from utility networks. To resolve these challenges, researchers have been investigating various aspects of EV charging including PEV load shifting to address the so called duck curve challenges associated with the rapid increase in demand at sunset [12], [13].

Recently, there has been a growing attention to use graph theory in many engineering applications (see [14]–[16]). This stimulates leveraging on the wealth of the fundamental graph related theories in modeling and synthesis of EV networks. Although EV community has recently utilized some aspects of graph theory in synthesizing EV networks [17]–[23], these works are not leveraging on substantial concepts of graph theory. In fact, previous studies have used graph topology for only visualizing the map of EV network. After constructing a graph-like EV network, they implement optimization techniques in different frameworks to address route planning [6]–[18], placement [19], and sizing [22] as well as simultaneous placement and sizing [23]–[25]. In [19], the locations of fast charging stations are attained according to the spatio-temporal requirements of the planners. Grasshopper optimization technique is implemented in [25] to address the placement and sizing of CSs where the EV battery load models are developed for load flow analysis. In [23], a real case optimal CS placement and sizing is addressed using five integer linear programs based on weighted set covering models of the CSs locations. Using a two stage optimization technique, the provision and dimension of DC fast charging stations are investigated with particular attention for maintaining the voltage stability by adding a minimum number of voltage stabilizers. A multi-objective particle swarm optimization method is used in [20] for the planning of charging stations. Similar to these studies, the majority of CS placement and sizing approacehs rely on an optimization tool. However, these computational tools are always subject to computationally interactable solutions [24]. The lack of an analytical approach to CS placement and sizing motivates leveraging on the potential of graph theoretic properties to establish a systematic method which is less affected by the computational burden. In this paper, we will show that graph theory can be used for modelling EV networks upon which the EV problems can be reformulated based on control frameworks where there are useful theories that can be adapted for placement and sizing of CSs.

This study proposes a new graph-based approach to modeling, synthesis, and analysis of EV networks that considers the impacts of traffic and is demonstrated for the placement and sizing of CSs based on the following steps: i) The EV network is modeled by a graph where the nodes are potential locations of CSs and edges represent the traffic (e.g., number of vehicles between the nodes). A model of network synchronization [27] is assumed as the EV network protocol. This model is then developed into a pinning framework [28] and [29] featuring actual CSs as the driver nodes. ii) The placement problem is mapped to the problem of finding a set of driver nodes for a CN representing the EV network. We verify that this set act as charging stations and can reduce the waiting time below a threshold level. Further, the problem of CSs sizing is reformulated as a problem of finding an optimal regulator gain. iii) The proposed approach is then elaborated by introducing a deployment strategy for portable charging stations (PCSs). This will compensate small mismatches between the generation and EV demand particularly during peak traffic hours. iv) Finally, the impacts of graph symmetry (or automorphism groups) on the graph of EV network are investigated. In particular, the role of symmetry in determining the number and location of charging stations is highlighted.

The proposed graph-based EV model facilitates addressing the EV network problems using various analytical approaches originated from control theories. The novel graph theoretic approach to EV network placement and sizing is relying on reformulation of these problems in a control framework. The study verifies that the charging stations can be considered

as the driver nodes of a complex network. Then the set of driver nodes (or CSs) and their control inputs (size of CSs) can be identified using established control theories. Inspired by the similarity of the structural dynamics of two nodes in the same automorphism (or generator of automorphism), this study verifies that these nodes can be alternatively selected as the charging spot. This feature is notable as the selected spots by placement approaches are subject to practical constraints.

As a comprehensive case study, the proposed method and all results are examined on the EV network of Perth in Western Australia. The main contributions and advantages of the proposed graph-based method for modelling, placement and sizing of CSs within EV networks are:

- Reformulating the problems of CSs placement and sizing to a control framework which facilitate using fundamental control and graph theories.
- Consideration of traffic flow and its impacts on EV network controllability, number, locations and sizes of CSs such that vehicle waiting times at all CSs are limited below a desirable threshold level.
- Investigating the graph symmetry of EV network and verifying its impact on number and locations of the CSs as well as providing alternative spots for CSs.
- A strategy for the deployment of PCSs in selected areas (subgraphs) is introduced and tested to further improve the quality of solutions by reducing the overshooting of the waiting times during peak traffic.

The rest of the paper is organized as follows. Section II presents some mathematical preliminaries on graph theory and graph symmetry. Section III discusses the main idea of the paper, introduces the proposed approach for placement and sizing of CSs and investigates the impacts of EV graph symmetry on the solutions. Simulations results are presented and analyzed in Section IV followed by the conclusion.

II. Preliminaries

A complex network can be abstracted by a graph $\mathcal{G}(V, E)$ where V and E characterize the set of nodes and edges, respectively. An edge exists between nodes i and j if $(i, j) \in E$. The graph is called undirected if the edges have no orientation. The adjacency matrix $\mathcal{A}$ of an undirected graph is a square $|V| \times |V|$ matrix whose element $[\mathcal{A}_{ij} = 1]$ if there is an edge between nodes i and j, and $[\mathcal{A}_{ij} = 0]$ when there is no edge. The *order* and the *size* of $\mathcal{G}$ are the cardinalities of its vertex set V and its edge set E, respectively.

A *permutation* σ on a set of nodes V is a bijection from V to itself, i.e., $\sigma : V \to V$. Through a permutation, the node sequence or order will be changed. The *order of permutation*, denoted by order(σ), is the smallest positive integer m such that $\sigma_1 \circ \sigma_2 \circ \cdots \circ \sigma_m = \sigma^m = \varepsilon$ where ε is the identity (trivial) permutation.

Definition 1: The composition or product of two functions ζ and δ, denoted by $\zeta \circ \delta$ is the pointwise action of ζ to the result of δ which generates a third function. The notation $\zeta \circ \delta$ is read as "ζ composed with δ". Intuitively, by composition of two functions, the pointwise output of the inner function becomes the input of the outer function. As an example, the Appendix explains how to compute the composition of two functions.

Graph symmetry is originated from discrete mathematics and can be revealed by automorphism groups. Automorphism is a permutation of graph to itself that preserves the graph structure, meaning the adjacency matrix of the underlying graph remains unchanged. As a result, nodes in the same automorphism have the same structural role in the graph. This type of symmetry has important implications for the controllability and robustness [30] of the underlying network [15], [16], [31], and [35], [36]. A formal definition of automorphism is as below.

An automorphism of $\mathcal{G}$ is a permutation σ for which $\{i, j\} \in E(\mathcal{G})$ if and only if $(\sigma(i), \sigma(j)) \in E(\mathcal{G})$. The automorphism group of $\mathcal{G}$ and its size are denoted by $Aut(\mathcal{G})$ and $|Aut(\mathcal{G})|$, respectively. Also, all automorphisms can be identified from a set of elementary automorphisms or generators of automorphisms $Gen(\mathcal{G})$. There are well known algorithms to compute graph automorphisms. There are also computing tools such as Sage (System for Algebra and Geometry Experimentation) and GAP (Graph Analytics Platform) for attaining $Aut(\mathcal{G})$ and $Gen\mathcal{G}$.

Definition 2: The graph $\mathcal{G}$ is symmetric if $Aut(\mathcal{G})$ contains at least one non-identity automorphism, otherwise it is called asymmetric. Identity permutation is also called trivial automorphism or trivial generator.

A set of nodes S of graph $\mathcal{G}$ is called determining set if every automorphism of $\mathcal{G}$ can be uniquely determined by its action on S. An element $s \in S$ is a fixed point of σ if $\sigma(s) = s$ where $\sigma : S \to S$ is a permutation of a set S. The permutation σ moves the point v if $\sigma(v) \neq v$. The fixed and moved points by the permutation σ are denoted by $\mathrm{Fix}(\sigma)$ and $\mathrm{Move}(\sigma)$, respectively. More details about graph symmetry can be found in [37].

III. EV Network Graph and Proposed Solution for Placement and Sizing of Charging Stations

This section establishes the main ideas of the paper upon reformulating the CS placement and sizing into a networked control problem which facilitates implementing control and graph theories. The CS placement is transformed to the problem of finding the set of driver nodes that will guarantee the full controllability of the EV network graph. CS sizing is then mapped to the problem of finding a set of optimal feedback gain in LQR (Linear Quadratic Regulator) framework. Also, a strategy for deploying of PCSs is proposed that will further improve the quality of the solution. Further, the symmetry of EV graph and its impact on the number and positions of CSs as well as its role in providing alternative spots for selected charging stations are verified.

A. EV Network Modeling and Problem Formulation

The EV network is modeled as a graph where nodes are positioned at the potential locations for CSs and the edges represent the number of vehicles in the area between the two corresponding nodes. A few spots along the roads are specified as the primary potential places for CSs. To determine

the number of vehicles on the main roads, some edges are assumed between nearby nodes according to the traffic flow. The edges are weighted based on the number of vehicles in the area. The waiting times at potential stations are considered as the system states. The dynamic equation of EV network can thus be formulated as

$$\dot{T}_i = -\sum_{j=1}^{n}\big(T_i - T_j\big) \quad (i = 1, \ldots, n) \tag{1}$$

where T is the system state and represents the waiting time. T_i is the state of i^{th} node. The above equation features typical synchronization protocol. Considering the control inputs as the charging supply in charging stations, the dynamic equation of the network can be written as below

$$\dot{T}_i = -\sum_{j=1}^{n}\big(T_i - T_j\big) + Bu(t) \quad (i = 1, \ldots, n) \tag{2}$$

where B is the input matrix and $u(t)$ is the control signal or charging supply injected through the CSs. Equation (2), which renders a general pinning protocol, provides a framework suitable for applying control theories.

Given the above formulation, CS placement and sizing problem can be restated as below.

Problem 1: Given the mathematical model of EV network in (2), find the set of driver nodes that can fully control the dynamic of (2).

Problem 2: Find the optimal control $u = -\mathcal{K}T$ for the set of driver nodes attained from the solution of *Problem 1*.

B. Proposed CS Placement Formulation and Solution

Based on the formulation presented in the previous section, the CS placement problem can be transformed to the problem of finding the required driver nodes that can fully control the complex network of (2). Then the attained driver nodes are correspondent to the positions of the required CSs.

The network dynamic in (2) can be rewritten as below

$$\dot{T}_i = -L(\mathcal{G})T_i + Bu(t) \quad (i = 1, \ldots, n) \tag{3}$$

where $L(\mathcal{G})$ is the Laplacian matrix and is given by

$$L(\mathcal{G}) = \Delta(\mathcal{G}) - \mathcal{A}(\mathcal{G}) \tag{4}$$

where $\Delta(\mathcal{G})$ and $\mathcal{A}(\mathcal{G})$ are the degree and adjacency matrices, respectively. Also, $T = (T_1, \ldots, T_N)^T$ represents the waiting time at each node, $\mathcal{A} \in \mathbb{R}^{N\times N}$ stands for the coupling or adjacency matrix of the system where its elements a_{ij} denote the weight of the link between i and j. B is the $N\times m$ control matrix where m stands for the number of controllers in the control vector $u = (u_1, \ldots, u_m)^T$. The dynamics in (3) is controllable if the pair $(-L(\mathcal{G}), B)$ is controllable [31].

To find the required driver nodes, the exact controllability method (ECM) is implemented [32]. The method is based on Popov-Belevitch-Hautus (PBH) rank criterion upon which the minimum number of driver nodes is equal to the maximum geometric multiplicity of all eigenvalues of the network matrix. Based on PBH theorem, the system (3) is fully controllable (meaning that the waiting time can be reduced to the desired values in finite time) if and only if

$$\operatorname{rank}(cI_N - L(\mathcal{G}), B) = N \tag{5}$$

is guaranteed for any complex number c, where I_N is the identity matrix. In [32], it is proven that the minimum number of driver nodes N_D can be calculated by the maximum geometric multiplicity $\mu(\lambda_i)$ of the eigenvalue λ_i of $L(\mathcal{G})$, that is

$$N_D = \max_i\{\mu(\lambda_i)\} \tag{6}$$

where

$$\mu(\lambda_i) = \dim V_{\lambda_i} = N - \operatorname{rank}(\lambda_i I_N - \mathcal{L}). \tag{7}$$

The minimum number of driver nodes for undirected networks can be determined by the maximum algebraic multiplicity $\delta(\lambda_i)$ of λ_i as

$$N_D = \max_i\{\delta(\lambda_i)\} \tag{8}$$

The control matrix B can be calculated from

$$\operatorname{rank}\big[\lambda^M - L(\mathcal{G}), B\big] = N \tag{9}$$

where λ^M is the maximum geometric multiplicity of the eigenvalue λ^M. Here, the attained non-zero entries of B imply on the necessity of injecting control input for those entries in order to fully control the network.

To find the minimum set of driver nodes, ECM implements elementary column transformation on the matrix $\lambda^M I - L(\mathcal{G})$ leading to a set of linearly independent rows. Eliminating all linear relations via B guarantees the full controllability with the minimum number of driver nodes. The minimum set of driver nodes attained by ECM characterizes the number and locations of CSs. These approaches are successfully implemented in Section IV for the EV network of Perth metropolitan and the results are presented in Figs. 2-5 and Table I.

C. Proposed CS Sizing Formulation and Solution

Once the CS placements are accomplished, the required capacity for each station must be determined. First, the EV network graph is partitioned into N_D subgraphs with only one charging station (determined in the previous section) in each subgraph. The partitioning algorithm, based on [33], decomposes the graph into N_D sub-graphs which will be refined later by making the final decomposition with as fewer interconnections as possible (see [33] for further details on the partitioning approach). Once the graph is partitioned, an adaption of Linear Quadratic Regulator (LQR) problem is implemented on each subgraph. The attained regulator will lead to the required capacity of the corresponding CSs.

For a dynamic system represented by the linear differential equations of (10), an optimal cost can be defined by the quadratic function of (11):

$$\dot{x} = Ax(t) + Bu(t), \tag{10}$$

$$J = \int_0^\infty \big(x^T Q x + u^T R u + 2x^T Y u\big)dt \tag{11}$$

where

$$u = -\mathcal{K}x \tag{12}$$

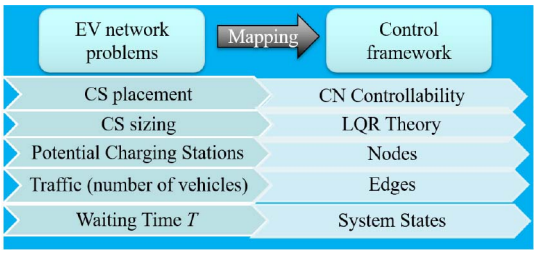

Fig. 1. Transformation of EV placement and sizing into control frameworks.

is the optimal feedback law and $\mathcal{K}$ is given by

$$\mathcal{K} = R^{-1}\left(B^T P + Y^T\right). \tag{13}$$

In (13), P is the solution of the following Riccati equation:

$$A^T P + PA - (PB + Y)R^{-1}\left(B^T P + Y^T\right) + Q = 0 \tag{14}$$

where Q, R, and Y are arbitrary symmetric and positive semi-definite matrices. In addition, (A, B) is stabilizable and $(Q - YR^{-1}Y^T, A - BR^{-1}Y^T)$ has no unsolvable modes on the imaginary axis. The relative importance of reducing and saving the control energy can be determined by the appropriate selections of Q and R. A higher R penalizes on the cost function demanding higher energy costs while a higher Q penalizes on the cost entailing higher settling time for the network.

Given the EV network model of (2), the problem of CS sizing can be transformed to the problem of finding the optimal control gain of (12). The following proposition facilitates this transformation.

Proposition 1: The required capacity $\mathcal{C}$ of the charging station located by applying ECM to CS placement is equal to

$$\mathcal{C} = \mathcal{K}T \tag{15}$$

where $\mathcal{K} = [k_1, k_2, \ldots, k_{n_s}]$ and $T = [T_1, T_2, \ldots, T_{n_s}]$ and n_s is the number of nodes in the graph. Further, $\mathcal{K}$ is given by (13) and P is the solution of the following Riccati equation

$$\mathcal{L}(\mathcal{G})^T P + P\mathcal{L}(\mathcal{G}) - PBR^{-1}B^T P + \mathcal{Q} = 0 \tag{16}$$

where

$$\mathcal{L}(\mathcal{G}) = L(\mathcal{G}) - BR^{-1}Y^T$$
$$\mathcal{Q} = Q - YR^{-1}Y^T.$$

Proof: In the LQR framework of the dynamic (3), parameter $\mathcal{K}$ attained from (13) minimizes the cost function of (11). By rewriting (12) as $u = \mathcal{C} = \mathcal{K}T$ and replacing matrix A with $\mathcal{L}$, P is the solution of the Riccati equation in (16). ■

The proposed EV placement and sizing transformations are illustrated in Figure 1. The Algorithm 1 summarizes the procedure for CS placement and sizing. In steps 1-9, we apply the exact controllability method to find the number of required CSs. Then to find the size of each CS, the whole graph is partitioned into N_D subgraphs where there is only one CS in each subgraph (steps 10-12). To attain an optimized balance between the sizes of CSs and reducing the peak of waiting times, the traffic models at 17 instances between 6 am and 10 pm have to be attained. in our case study, we attained this information (the number of vehicles) from the traffic map

Algorithm 1 A Graph-Based Solution to the CS Placement and Sizing Problem in EV Networks

Input: The traffic flow of the underlying area from 6 am to 10 pm (17 traffic flow models, one at every hour)
Output: Locations and sizes of CSs

1: **while** maximum iteration is not met **do**
2: Calculate the matrix B from rank$[\lambda^M - L(\mathcal{G}), B] = N$.
3: Assign $N_D = 0$.
4: **for** i=1 to N **do**
5: **if** $B(i)$=1 **then**
6: Assign a charging station to node i.
7: $N_D = N_D + 1$.
8: **end if**
9: **end for**
10: Apply partitioning algorithm to EV network to drive N_D subgraphs featuring one driver node per partition.
11: **for** i=1 to N_D **do**
12: Augment the subgraph by adding the detailed dynamics of the underlying area.
13: **for** t=1 to 17 **do**
14: Compute P from the Riccati equation $\mathcal{L}(\mathcal{G})^T P + P\mathcal{L}(\mathcal{G}) - PBR^{-1}B^T P + \mathcal{Q} = 0$.
15: Compute $\mathcal{K}_{it}$ from $\mathcal{K}_{it} = R^{-1}(B^T P + Y^T)$.
16: Assign the weighting factor ρ_i.
17: Compute $C_{it} = \rho_i \mathcal{K}_{it} T^*_{it}$.
18: **end for**
19: Compute $C_i = \frac{(C_{i1} + C_{i2} + \ldots + C_{i17})}{17}$
20: **end for**
21: Assign the weighing parameter q.
22: **for** i=1 to N_D **do**
23: **for** t=1 to 17 **do**
24: **if** $C_i < q\mathcal{K}_{it}T^*_{it}$ **then**
25: Assign a portable charging station (PCS).
26: **end if**
27: **end for**
28: **end for**
29: **end while**

of Western Australia [38]. In practice, T is a dynamic variable. Thus, in this paper, the attained capacity at each hour is weighted by a factor ρ_i where i represents the instant i (see steps 16-17 of Algorithm 1). For any small mismatch between the supplied capacity and charging demand, a portable charging station can be deployed. This means that given $\mathcal{K}_{it}$ and T^*_{it} as the optimal gain and waiting time of node i at hour t, a portable charging station will be deployed at the area covered by subgraph i if

$$C_i < q\mathcal{K}_{it}T^*_{it} \tag{17}$$

where C_i is the size (or capacity) of station i in kW and $0 < q < 1$ is an arbitrary weighting factor.

Note that the arbitrary weights R, Q, and Y can be selected accordingly to set the importance of either optimal size or the settling times of the system. The settling times are the amount of time it takes to reach to the desired system state. By selecting a big matrix Q the system reaches to the desired state rapidly in the cost of increased control signal $u(t)$. Similarly,

selecting a big matrix R leads to much smaller $u(t)$ but the system response will be much slower. Equivalently, selecting a big enough Q leads to non-optimal sizes for the CS while selecting a bigger matrix R reduce the capacity in the cost of increased time response to reach to the desired waiting time. Therefore a trade off is necessary while selecting theses weights. This illucidates how the waiting time and the size are affected by the solution of LQR.

D. Impact of Graph Symmetry on CS Placement Solution

Symmetry, described by graph automorphisms, plays an important role in the controllability of complex networks [31], [34], and [35]. Symmetry is an obstruction to controllability, meaning a big automorphism group necessitates a high number of driver nodes [35]. Therefore, the possible impacts of EV network symmetry on the number and positions of the required charging stations can be investigated by mapping the CS placement problem to the CN controllability problem. The placement of CSs is affected by the automorphism groups. The cardinality (size) of automorphism group determines the symmetry strength of a graph. It is verified in [35] that the symmetry is an obstruction to controllability, meaning a higher number of driver nodes (or in our case, charging stations) are required to fully control the network when the size of automorphism group is big. Lemma 1 relates CN controllability to automorphism group.

Lemma 1: Assume that $A(\mathcal{G})$ is diagonalizable and symmetry preserving [36], then the pair $(A(\mathcal{G}), B(S))$ is uncontrollable if $\mathcal{G}$ admits a nontrivial automorphism σ which fixes the input set S, i.e., $\sigma(i) = i$ for all $i \in S$.

In practice, due to difficulty of listing and sweeping all automorphisms of medium/large networks such as the EV networks, the above lemma is not computationally effective. In [14], an alternative approach based on generators of automorphisms is presented which impose less computation burden.

Lemma 2 [14]: Assume that $A(\mathcal{G})$, the adjacency matrix of the underlying network, is diagonalizable and symmetry preserving and B is the input matrix applied to set S of N_d driver nodes. Then, the necessary conditions for controllability of the pair $(A(\mathcal{G}), B(S))$ are

(i) $\sigma_{g_t}(i) \neq i$ and for all $i \in S$ and $t = 1, 2, \ldots, h$, where $\sigma_{g_t}(i)$ represents for the set of generators and $h = |Gen(\mathcal{G})|$,

(ii) $S(i) \neq j$ for the set of pairwise joint generators with joint node j where $i = 1, 2, \ldots, N_d$,

(iii) if all nodes of generators g_k are joint nodes then all of its joint nodes are in S.

The above lemma leverages on some properties of permutation products to find the determining set of a graph. Then by mapping the Lemma 1 to CS placement problem, a set of necessary conditions for finding the number and positions of charging stations can be attained. This lemma is used in the simulations of Section IV to investigate the impact of symmetry on EV network of Perth, Western Australia.

An important feature of Lemma 2 for EV networks is that it provides alternative locations for the charging stations. This fortunate feature is attained since the determining set is not unique. Therefore, it is possible to replace one node in S with another node that has the same structural role in the EV network graph. Two (or more) nodes in a given generator can have the same dynamic in the graph meaning that replacing the entire corresponding to these two nodes in the graph adjacency (or Laplacian) matrix will not change the adjacency (or Laplacian) matrix. This feature is important for EV networks due to geographical limitations on selecting a spot for CS as the selected spot by ECM or other approaches might not be authorized for constructing a charging station.

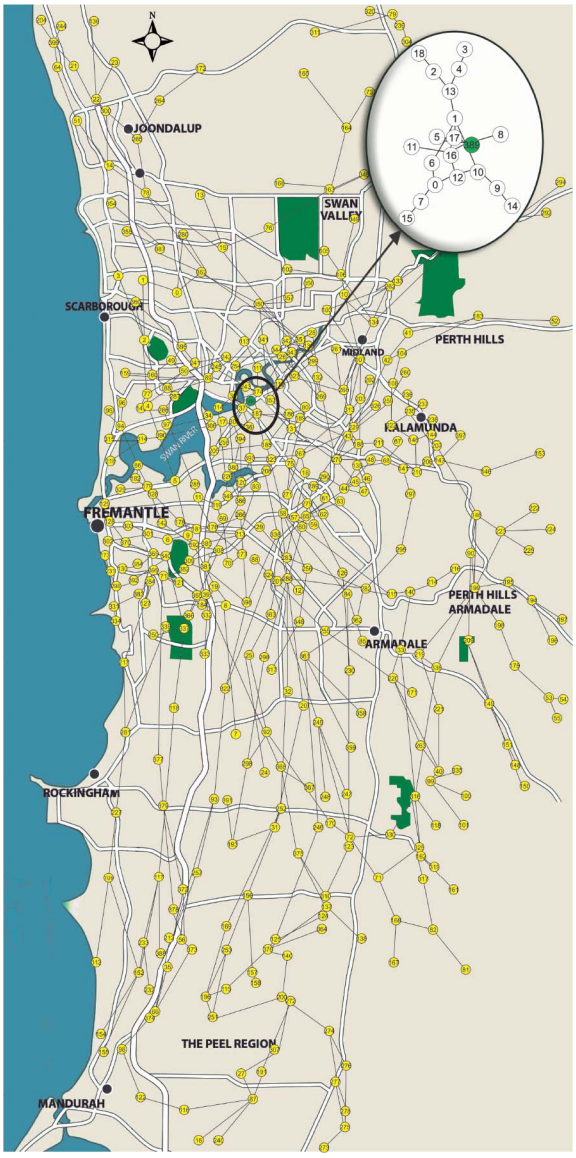

Fig. 2. Map of Perth metropolitan in Western Australia with 400 virtual nodes representing the potential candidate locations for CSs. The magnified area represents the augmented dynamics of the selected subgraph featuring node 389 as its charging station (driver node). There are 39 more subgraphs that are not shown due to space limitations.

IV. Case Study: EV Network of the Perth Metropolitan in Western Australia

The proposed graph-based approaches for the modeling of EV networks and finding locations/sizes of the CSs and

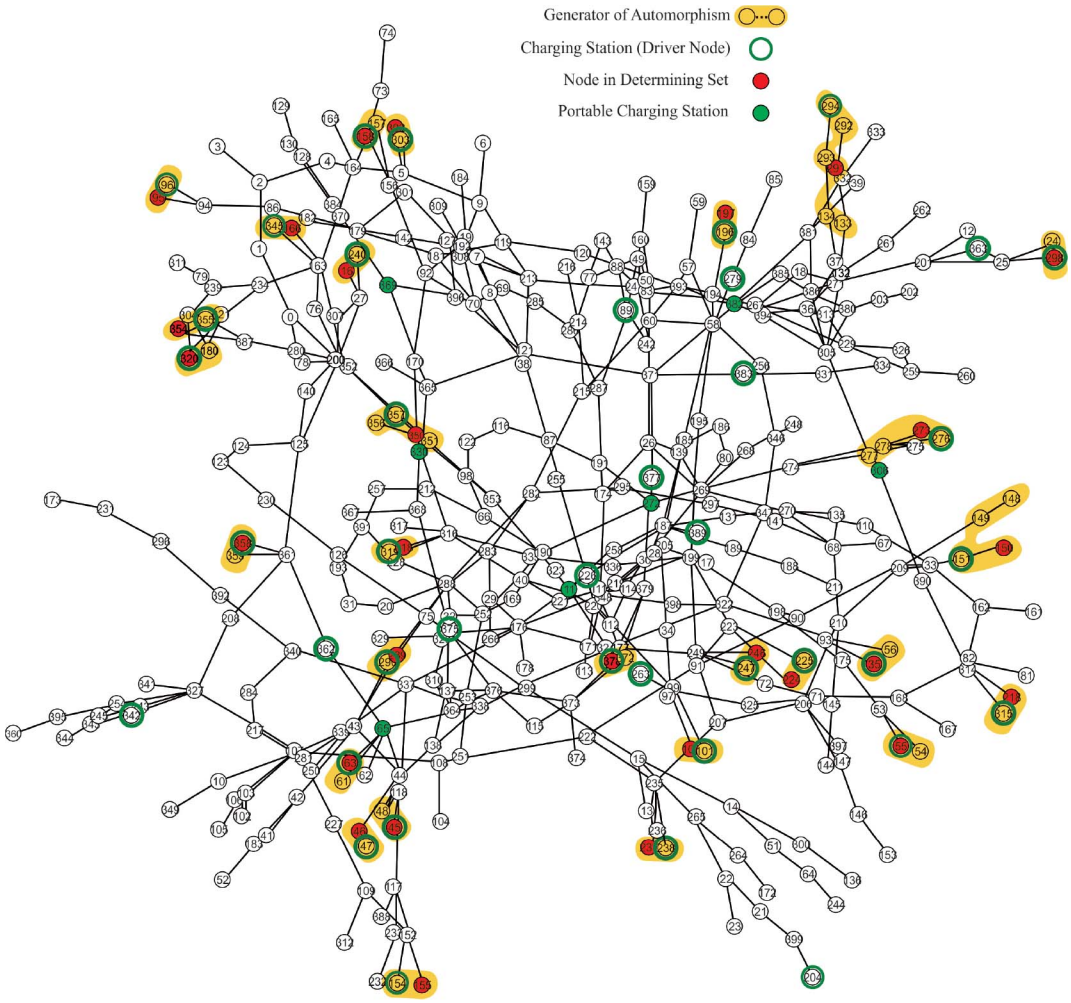

Fig. 3. Generated graph of Perth EV network showing locations of the 40 CSs or driver nodes (green rings), the 28 generators of automorphisms (black circles in yellow highlighted areas), the 7 PCS nodes (green circles), and the 28 nodes in the determining set (red circles). There are 400 virtual nodes (Fig. 2). The 28 nodes in determining set are also in CSs set.

PCSs are implemented and tested on the EV network of Perth Metropolitan in Western Australia (Figure 2) and the results are provided in Figure 3-5 and Table I. This section provides detailed explanation and analyses of the generated simulation results.

A. Graph and Parameters of Perth EV Network

The graph of Figure 2 is generated based on the traffic information of Perth metropolitan taken from the Traffic Map of Western Australia [38] which measures the number of vehicles on the main roads. The nodes (potential locations for CSs) are selected using the actual traffic map between areas with known traffic where the number of vehicles in each area represents the weight of the edge connecting two nearby areas. The Perth EV network is bordered to the north by city of Wanneroo, to the east by City of Swan, Kalamunda, and Armadale, and is bordered to the south by Mandurah and to the west by Indian Ocean.

For the simulations and analysis of this paper, we have made a number of assumptions including 1) there are $10,000$ vehicles in Perth metropolitan, WA with an average vehicle power consumption of 0.173 kW/km [38], 2) all CSs are equipped with the standard DC fast chargers with the service time of $10-15$ minutes [17], 3) the desired waiting time is the same at all CSs and is limited to the threshold of 15 minutes, 4) the maximum and minimum battery state of charge for EVs are SoCmax $=$ 80% and SoCmin $=$ 20%, 5) EVs arriving at the CSs have uniform SoC distribution in the range of 20% to 80%. Considering the characteristics of the existing commercial vehicles, the upper and lower boundaries of SoC are fixed at ideal level, which are currently 80% for the maximum level and 20% for the minimum level [39].

B. Number, Locations and Sizes of CSs of Perth EV Network

To find the number and locations of CSs, the set of driver nodes that can fully control the EV network (represented by (2)) must be determined. To this end, the exact controllability method is implemented (Equations (5)-(9)) in MATLAB which resulted in a set of 40 driver nodes as illustrated in Figure 3 with green rings. The ECM relates the controllability of complex networks to the maximum geometric multiplicity of eigenvalues of the matrix A, and in turn, to the

TABLE I
SUMMARY OF SIMULATION RESULTS FOR THE PERTH EV NETWORK OF FIGURE 2-3

Parameter	**Value**	**Figure number and/or Descriptions**
Virtual Nodes	400	Figure 2, yellow highlighted groups of nodes.
Aut($\mathcal{G}$)	268 m	The 268 million automorphisms are identified with the Sage software package.
Gen($\mathcal{G}$)	28	Figure 2, yellow highlighted groups of nodes; $Gen(\mathcal{G})$ =[(372,378), (358,359), (350,351)(356,357), (318,319), (302,303), (289,290), (273,276), (277,278), (246,247),(237,238), (224,225), (218,315),(196,197), (180,320), (166,345), (157,158), (154,155), (100,101), (35,56), (148,150)(149,151), (95,96), (354,355), (133,134)(291,293)(292,294), (61,63), (54,55), (46,47), (45,48), (24,298), (16,240)].
CSs	40	Figure 3, green rings at nodes 35 (275 kW), 45 (128 kW), 47 (213 kW), 55 (349 kW), 63 (72 kW), 89 (200 kW), 96 (173 kW), 101 (362 kW), 151 (252 kW), 154 (393 kW), 158 (234 kW), 196 (336 kW), 204 (188 kW), 225 (218 kW), 226 (72 kW), 238 (254 kW), 240 (385 kW), 247 (214 kW), 263 (192 kW), 276 (317 kW), 279 (87 kW), 290 (352 kW), 294 (52 kW), 298 (205 kW), 303 (271 kW), 315 (226 kW), 319 (191 kW), 320 (128 kW), 342 (241 kW), 345 (365 kW), 355 (273 kW), 357 (379 kW), 358 (90 kW), 362 (204 kW), 363 (94 kW), 375 (218 kW), 377 (276 kW), 378 (59 kW), 383 (311 kW), and 389 (371 kW).
PCSs	7	Figure 3, green circles, nodes 11, 65, 272, 306, 330, 369, and 382 (PCSs have the same capacity of 250 kW).
Determining Set $\mathcal{S}$	28	Figure 2, red circles at nodes 16, 35, 45, 46, 55, 63, 95, 100, 150, 155, 158, 166, 197, 218, 224, 237, 246, 273, 289, 291, 298, 302, 318, 320, 350, 354, 358, and 372.
Nodes in both sets of S and CSs	28	Figure 3, 28 nodes in the determining set that are also in the set of CSs.
Waiting Times at CSs without PCSs	-	Figure 4, the family of 40 curves with a daily average of 12 minutes and two peaks of 19.3 minutes and 17 minutes. The average waiting times at peak hours, 9 am and 4 pm, are 17.7 and 17.1 minutes, respectively.
Waiting Times at CSs with PCSs	-	Figure 5, the family of 40 curves with a daily average of 12 minutes. Two peaks of Fig. 4 have reduced to 16.6 minutes and 16.5 minutes. Also, the average waiting times at peak hours have reduced to 15.4 and 15.35 minutes.

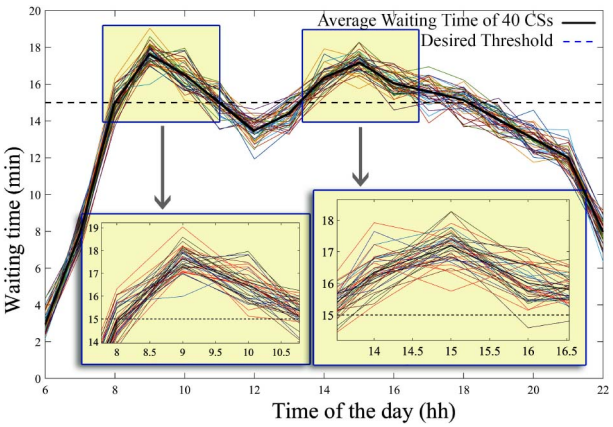

Fig. 4. Waiting time at the allocated 40 CSs (Table I; row 5) without the deployment of PCSs. The thick black curve shows the average waiting time of the 40 CSs from 6 am to 10 pm.

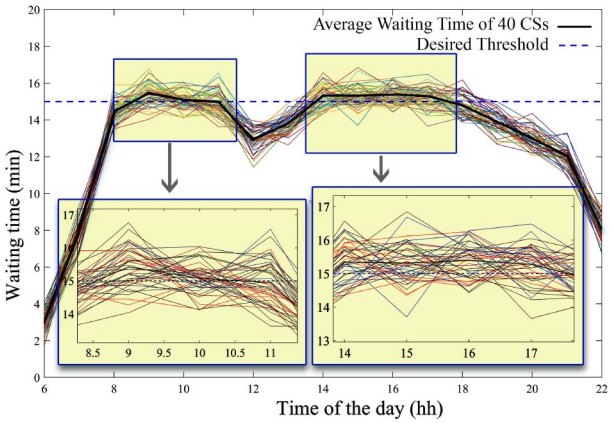

Fig. 5. Waiting time at the allocated 40 CSs (Table I; row 5) with the deployment of PCSs (Table I, row 6) according to Steps 21-28 of Algorithm 1. The thick black curve shows the average waiting time of the 40 CSs from 6 am to 10 pm.

corresponding Laplacian matrix $L(\mathcal{G})$. This matrix, in the context of EV network, is the adjacency matrix representing the traffic flow between nearby nodes. According to Section III-B, the driver nodes that can fully control a complex network are mapped into the charging stations that can fully supply the charging demand of EV network. Due to analogy between driver nodes and charging stations, these driver nodes can thus be selected as the locations of the CSs. Therefore, using the Algorithm 1, the number and locations of charging stations can be attained from steps 2-9.

To find the size of each CS, first the 400-node graph in Figure 2 is partitioned into 40 sub-graphs with minimum edge cuts. The graph partitioning is accomplished according to step 10 of Algorithm 1. This is constrained by the consideration of only one CS in each subgraph. The LQR approach is then implemented in MATLAB for each subgraph after subgraph augmentation (steps 12-15). Due to space limitation, only one of the subgraphs corresponding to the CS at node 389 is augmented in Figure 2. The arbitrary weights R, Q, and Y for each subgraph are selected after a few trials and errors. Once these arbitrary weights are selected, the Riccati equation in step 14 can be solved where B in step 14 has only one non-zero element at the entry corresponding to the driver node (or charging station) and L corresponds to the Laplacian matrix of traffic flow in the subgraph. The solution of the Riccati Equation (in step 16) is the matrix P which is then substituted in step 15 to attain $\mathcal{K}$. Finally, according to Proposition 1, the required capacity for the corresponding CS in the subgraph can be computed from step 19. Note that the augmented area contains more nodes (not shown in Figure 2) that are used to accurately model the traffic flow of the area. The corresponding subgraph to the CS at node 389 is magnified in Figure 2 to illustrate the detailed dynamics of the underlying area. According to Algorithm 1, the LQR approach is implemented for this subgraph for 17 instances corresponding to 17 traffic models between 6 am and 10 pm. These models are each investigated to attain the required capacity at

each hour (steps 13-17 of Algorithm 1). Solving the LQR for 17 instances has resulted in the following capacities at each hour (ordered form 6 to 10 pm, respectively).

$$C_{it} = [339, 391, 472, 498, 475, 455, 431, 411, 440, 465, 457, 432, 398, 372, 341, 299, 273] \quad (18)$$

Steps 18-28 of Algorithm 1 facilitate attaining an optimized charging capacity via choosing an appropriate parameter ρ. The arbitrary weighting parameter ρ (where $0 < \rho_i < 1$) determines the balance between reducing the overshoot in the waiting time at peak hours and increasing the charging capacity. In fact, if for all values of i we assume $\rho_i = 1$ then the overshoot at peak hours will be zero at the cost of significant increase in charging capacity. According to the magnitude difference between the charging demand at peak hours and the rest of instances, we selected the variable values for ρ_i (e.g., $\rho_i \approx 1$ at peak hours). This has resulted to the required charging capacity of 371 kW at node 389. Similarly, the required charging capacities of other CSs are calculated and provided in Table I (row 5).

C. Waiting Times of Perth EV Network Without Portable Charging Stations

To find the waiting times, the EV network is simulated with the 40 allocated CSs (driver nodes) of Figure 3 and the calculated CS capacities of Table I (row 5). The EV network dynamic taken from (3) is modeled by selecting initial waiting times at each station while matrix B and the capacities (corresponding to control signal $u(t)$ in (3)) are computed in the previous section. Equation (3) is simulated in MATLAB and the network states (waiting time T_i at each station) over the 17 instants models between 6 am and 10 pm are calculated as illustrated in Figure 4. As indicated in this figure, the waiting time diagrams undergo two overshoots near the peak hours. This is caused by selecting different ρ_i for different hours. Although the waiting time has increased at peak hours, the network capacity is optimized. For example, if $\rho_i = 1$ for all values of i then the charging capacity at node 389 must be 495 kW which is 124 kW more than the computed capacity (371 kW) in the previous section.

D. Introduction of PCSs in Perth EV Network

As illustrated in Figure 4, there are some overshoots during peak traffic hours around 9 am and 3 pm (e.g., the waiting times are longer than the designated threshold of 15 minutes). These overshoots are mainly due to the selected weighting factor (ρ_i; Algorithm 1: Step 17). This paper proposes deployment of PCSs to reduce the overshoots. The deployment of PCSs can be scheduled by i) updating the waiting time vector every hour, ii) checking inequality (17), and iii) proceeding with Steps $21 - 28$ of Algorithm 1. For the EV network of Figure 2, seven PCSs are assigned and located in an hourly basis (Table I, row 6). Adding these PCSs modifies the network dynamics by changing the entries of matrix B associated to the nodes corresponding to the locations of the added PCSs. Running the EV network model of (3) in MATLAB and measuring the new waiting times at the 40 charging stations has resulted in shorter waiting times at peak hours as illustrated in Figure 5. Compared with the results of Figure 4, there are notable reductions in the frequency and magnitudes of the overshoots.

E. Analyses of Simulation Results for Perth EV Network

A symmetry analysis of the EV network of Perth is performed with Sage software package. Having the network Laplacian matrix L, the number of automorphisms of the EV network can be attained in Sage in less than a minute by simply typing a one line command (i.e., by typing "*G.automorphism_group()*" where G is the simulated network by its Laplacian). This has resulted in approximately 268 million automorphisms. Obviously, it is not computationally effective to sweep over all automorphisms. Instead, the generators of automorphisms are calculated using the command "*gens(G)*" which is resulted in 28 generators listed in Table I (row 4) and illustrated in Figure 3. As indicated in Figure 3, there is at least one CS in each generator set. This verifies the adaption of Lemma 1 to EV networks where driver nodes represent the charging stations. According to Lemma 2, a determining set can be calculated by sweeping over the set of 28 generators and selecting one node in each generator. The determining set thus contains 28 nodes (Figure 3; red circles) that are listed in Table I, row 7.

The concept of determining set characterizes an important feature for the CS placement problem. Since the determining set of an automorphism group is not unique, there are alternatives for the majority of driver nodes to act as the charging stations. For example, node 378 in the determining set (Figure 3) can be replaced with nodes 372 because the set of nodes $\{372, 378\}$ is a generator in $Gen(\mathcal{G})$ (Table I, row 4) and as a result they can play the same structural role in the EV network.

The set of driver nodes together with the generators of automorphisms are illustrated in Figure 3. Also the set of nodes belonging to the determining set is highlighted in Figure 3. There is an overlap between the set of driver nodes and determining set meaning that all nodes in the determining set also belong to the set of driver nodes. This implies the importance of symmetry in the structure of EV network. In practice, all locations selected as driver nodes may not be suitable for the installation of charging stations. Fortunately, the determining set provides alternative options/locations for the installation of charging station.

V. Conclusion

A graph-based method is proposed and implemented for the placement and sizing of CSs that considers traffic and limits the vehicle waiting times at all stations below a desirable threshold level (e.g., 15 minutes). The research reveals the analogies between (i) the CS placement and controllability of the underlying network and (ii) the CS sizing and optimal controller design. In addition, a strategy for deployment of PCSs is introduced to further improve the quality of solutions by reducing the overshooting of waiting times during peak traffic hours. Although further study is required to analytically

explain the symmetry impacts of EV networks on the solutions of CS placement and sizing, our results verifies that the EV graph symmetry, in the context of graph automorphism, can significantly change the number and locations of the CSs while suggesting alternative locations for CSs.

The new proposed framework to reformulate CS placement and sizing using control and graph theories facilitates adapting many other concepts from control as well as graph theory. Our future work will be on the development of robust control methods to EV networks under dynamic pricing and uncertain traffic. Another interesting research direction would be pursuing an analytical explanation for the overlap between the determining set (attained with symmetry analysis of the underlying network) and the set of driver nodes (or charging stations). Finally, the impact of the proposed charging network design on the power grid is not considered in this paper and will be addressed in our further research.

APPENDIX
COMPOSITION OF PERMUTATIONS

The method of calculating the product or composition of two permutations is described below through an example.

Example A.1: Let ζ and δ be given by

$$\zeta = (1 \quad 2 \quad 3 \quad 4 \quad 5) \quad \textit{and} \quad \delta = (1 \quad 4 \quad 3).$$

To compute the composition of ζ and δ, $\zeta \circ \delta$, first we have to check the commutation (represented by the symbol $\mapsto$) of element by δ and then its commutation by ζ. In this example

$$\begin{aligned}
1 &\mapsto^{\delta} 4 \mapsto^{\zeta} 5 \Rightarrow \zeta \circ \delta(1) = 5 \\
5 &\mapsto^{\delta} 5 \mapsto^{\zeta} 1 \Rightarrow \zeta \circ \delta(5) = 1 \\
4 &\mapsto^{\delta} 3 \mapsto^{\zeta} 4 \Rightarrow \zeta \circ \delta(4) = 4 \\
3 &\mapsto^{\delta} 1 \mapsto^{\zeta} 2 \Rightarrow \zeta \circ \delta(3) = 2 \\
2 &\mapsto^{\delta} 2 \mapsto^{\zeta} 3 \Rightarrow \zeta \circ \delta(2) = 3.
\end{aligned}$$

Thus the composition of ζ and δ is $\zeta \circ \delta = (1 \quad 5)(3 \quad 2)$.

REFERENCES

[1] N. Daina and J. W. Polak, "Hazard based modelling of electric vehicles charging patterns," in *Proc. IEEE Conf. Expo. Transport. Elect. Asia–Pac. (ITEC AsiaPacific)*, 2016, pp. 479–484.

[2] E. Daramy-Williams, J. Anable, and S. Grant-Muller, "A systematic review of the evidence on plug-in electric vehicle user experience," *Transport. Res. D Transp. Environ.*, vol. 71, pp. 22–36, Jun. 2019.

[3] S. Ou, Z. lin, X. He, S. Przesmitzki, and J. Bouchard, "Modeling charging infrastructure impact on the electric vehicle market in China," *Transport. Res. D Transp. Environ.*, vol. 81, p. 2020, Apr. 2018.

[4] *Community Energy Association*. Accessed: Feb. 20, 2020. [Online]. Available: http://communityenergy.bc.ca/

[5] S. Huang, L. He, Y. Gu, K.Wood, and S. Benjaafar, "Design of a mobile charging service for electric vehicles in an urban environment," *IEEE Trans. Intell. Transp. Syst.*, vol. 16, no. 2, pp. 787–798, Apr. 2018.

[6] Z. Moghaddam, "Smart charging strategies for electric vehicle charging stations," Ph.D. dissertation, School Eng., Edith Cowan Univ., Joondalup, WA, Australia, 2019.

[7] Q. Liu *et al.*, "Planning mobile charging vehicles based on user charging behavior," in *Proc. ACM*, Jun. 2018, pp. 37–42.

[8] S. N. Yang, H. W. Wang, C. H. Gan, and Y. B. Lin, "Mobile charging information management for smart grid networks," *Int. J. Inf. Manag.*, vol. 33, no. 2, pp. 245–251, 2013.

[9] S. F. Tie and C. W. Tan, "A review of energy sources and energy management system in electric vehicles," *Renew. Sustain. Energy Rev.*, vol. 20, pp. 82–102, Apr. 2013.

[10] J. Li, J. Jiao, and Y. Tang, "An evolutionary analysis on the effect of government policies on electric vehicle diffusion in complex network," *Energy Policy*, vol. 129, pp. 1–12, 2019.

[11] B. N. E. Finance. (2017). *Electric Vehicle Outlook*. [Online]. Available: https://about.bnef.com/electric-vehicle-outlook

[12] H. Zhang, C. J. R. Sheppard, T. E. Lipman, T. Zeng, and S. J. Moura, "Charging infrastructure demands of shared-use autonomous electric vehicles in urban areas," *Transport. Res. D Transp. Environ.*, vol. 78, Jan. 2020, Art. no. 102210.

[13] Y. Huang and K. M. Kockelman, "Electric vehicle charging station locations: Elastic demand, station congestion, and network equilibrium," *Transport. Res. D Transp. Environ.*, vol. 78, Jan. 2020, Art. no. 102179.

[14] H. Parastvand, A. Chapman, O. Bass, and S. Lachowicz, "A symmetry perspective on complex network controllability with applications to power systems," *Power Elect. Syst. Res.*, to be published.

[15] B. D. MacArthur, R. J. Sanchez-Garcia, and J. W. Anderson, "Symmetry in complex neworks," *Discr. App. Math.*, vol. 156, no. 18, pp. 3525–3531, 2018.

[16] L. M. Pecora, F. Sorrentino, A. M. Hagerstorm, T. E. Murphy, and R. Roy, "Cluster synchronization and isolated desynchronization in complex networks with symmetries," *Nat. Commun.*, vol. 5, p. 4079, Jun. 2014.

[17] Z. Moghaddam, I. Ahmed, D. Habibi, and M. Masoum, "A coordinated dynamic pricing model for electric vehicle charging stations," *IEEE Trans. Transport. Electrific.*, vol. 5, no. 1, pp. 226–238, Mar. 2019.

[18] M. Baum, J. Dibbelt, T. Pajor, and D. Wagner, "Dynamic time dependent route planning in road networks with user preferences," in *Proc. 15th Int. Symp. Exp. Algorithms (SEA)*, vol. 9685, 2016, pp. 33–49.

[19] I. Morro-Mello, A. Padilha-Feltrin, J. D. Mello, and A. Calvino, "Fast charging stations placement methodology for electric taxis in urban zones," *Energy*, vol. 188, Dec. 2019, Art. no. 116032.

[20] Y. Zhang, Q. Zhang, A. Farnoosh, S. Chen, and Y. Li, "GIS-based multi-objective particle swarm optimization of charging stations for electric vehicles," *Energy*, vol. 169, pp. 844–853, Feb. 2019.

[21] B. Moritz, S. Jong, W. Dorothea, and Z. Tobias, "Consumption profiles in route planning for electric vehicles: Theory and applications," in *Proc. 16th Int. Symp. Exp. Algorithms (SEA)*, 2017.

[22] S. D. Gaikwad and P. C. Ghosh, "Sizing of a fuel cell electric vehicle: A pinch analysis-based approach," *Int. J. Hydrogen Energy*, vol. 45, no. 15, pp. 8985–8993, 2020.

[23] S. Boug and S. Layeb, "Determining optimal deployment of electric vehicles charging stations: Case of Tunis City, Tunisia," *Case Studies Transp. Policy*, vol. 7, no. 3, pp. 628–642, 2019.

[24] M. E. Kabir, C. Assi, H. Alameddine, J. Antoun, and J. Yan, "Demand aware deployment and expansion method for an electric vehicles fast charging network," in *Proc. IEEE Int. Conf. Smart Grid Commun. (SmartGridComm)*, 2019, pp. 1–7.

[25] S. R. Gampa, K. Jasthi, P. Goli, D. Das, and R. C. Bansal, "Grasshopper optimization algorithm based two stage fuzzy multiobjective approach for optimum sizing and placement of distributed generations, shunt capacitors and electric vehicle charging stations," *J. Energy Stor.*, vol. 27, Feb. 2020, Art. no. 101117.

[26] Y. Chen, S. Kar, and J. M. F. Moura, "Optimal attack strategies subject to detection constraints against cyber-physical systems," *IEEE Trans. Control Netw. Syst.*, vol. 5, no. 3, pp. 1157–1168, Sep. 2018.

[27] C. Chen, K. Xie, F. L. Lewis, S. Xie, and A. Davoudi, "Fully distributed resilience for adaptive exponential synchronization of heterogeneous multiagent systems against actuator faults," *IEEE Trans. Autom. Control*, vol. 64, no. 8, pp. 3347–3355, Aug. 2019.

[28] N. Ma, Z. Liu, and L. Chen, "Synchronisation for complex dynamical networks with hybrid coupling time-varying delays via pinning adaptive control," *Int. J. Syst. Sci.*, vol. 50, no. 8, pp. 1661–1676, 2019.

[29] Y. L. Huang and S. X. Wang, "Synchronisation in an array of spatial diffusion coupled reaction diffusion neural networks via pinning control," *Int. J. Syst. Sci.*, vol. 49, no. 5, pp. 1103–1118, 2018.

[30] H. Parastvand and M. J. Khosrowjerdi, "A new data driven approach to robust PID controller synthesis," *Int. J. Syst. Sci.*, vol. 46, no. 7, 2015, pp. 84–93.

[31] A. Chapman and M. Mesbahi, "On symmetry and controllability of multi-agent systems," in *Proc. 53rd IEEE Conf. Decis. Control*, 2014, pp. 625–630.

[32] Z. Yuan, C. Zhao, Z. Di, W. X. Wang, and Y. C. Lai, "Exact controllability of complex networks," *Nat. Commun.*, vol. 4, p. 2447, Sep. 2013.

[33] C. Ocampo-Martinez, S. Bovo, and V. Puig, "Partitioning approach oriented to the decentralised predictive control of large-scale systems," *J. Process Control*, vol. 21, no. 5, pp. 775–786, 2011.

[34] C. O. Aguilar and B. Gharesifard, "A graph-theoretic classification for the controllability of the Laplacian leader–follower dynamics," in *Proc. 53rd IEEE Conf. Decis. Control*, Los Angeles, CA, USA, 2014, pp. 619–624.
[35] A. Rahmani, M. Mesbahi, and M. Egersted, "Controllability of multi-agent systems from a graph-theoretic perspective," *SIAM J. Control Opt.*, vol. 48, no. 1, pp. 162–186, 2009.
[36] A. Chapman, M. Nabi-Abdolyousefi, and M. Mesbahi, "Controllability and observability of networks-of-networks via cartesian products," *IEEE Trans. Autom. Control*, vol. 59, no. 10, pp. 2668–2679, Oct. 2014.
[37] L. W. Beineke and R. J. Wilson, "Topics in algebraic graph theory," in *Encyclopedia of Mathematics and Its Applications*. Cambridge, U.K.: Cambridge Univ. Press, 2007.
[38] *Traffic Map of the Main Roads of Western Australia*. Accessed: Feb. 20, 2020. [Online]. Available: https://www.trafficmap.mainroads.wa.gov.au/map
[39] V. del Razo and H.-A. Jacobsen, "Smart charging schedules for highway travel with electric vehicles," *IEEE Trans. Transport. Electrific.*, vol. 2, no. 2, pp. 160–173, Jun. 2016.

Hossein Parastvand (Student Member, IEEE) received the B.S. degree in instrumentation and control from the Shiraz University of Technology, Shiraz, Iran, in 2008 and the M.S. degree in control engineering from the Sahand University of Technology, Tabriz, Iran, in 2010. He is currently pursuing the Ph.D. degree with the Smart Energy Systems Group, Edith Cowan University, Joondalup, WA, Australia. From 2010 to 2017, he was a Senior Automation and Control Engineer with MegaTrans Company, Iran. His main research focus is on the applications of control theories in complex power networks.

Valeh Moghaddam (Member, IEEE) received the Ph.D. degree in computer systems from Edith Cowan University, Joondalup, WA, Australia, in 2019. She is currently a Lecturer with the School of Information Technology, Deakin University, Geelong, VIC, Australia. Her current research interests include the management of smart grid and renewable energy systems with a focus on electric vehicles applications.

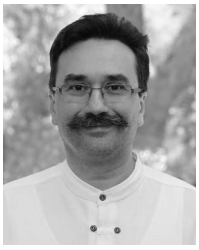

Octavian Bass received the undergraduation and Ph.D. degrees from the Politehnica University of Timisoara, Romania, in 1995 and 2001, respectively. His employment history includes research positions with the Budapest University of Technology and Economics, Hungary, Hong Kong Polytechnic University, Hull University, U.K., and Utsunomiya University, Japan. He was a Lecturer with James Cook University, Australia, from 2006 to 2009, and he is currently a Senior Lecturer with the School of Engineering, Edith Cowan University, Perth, WA, Australia. He has coauthored 90 professional publications. His fields of interest include smart grid technologies, renewable energy resources, and non-linear dynamics in power electronics.

Mohammad A. S. Masoum (Senior Member, IEEE) received the B.S. and M.S. degrees in electrical and computer engineering from the University of Colorado at Denver, Denver, CO, USA, in 1983 and 1985, respectively, and the Ph.D. degree in electrical and computer engineering from the University of Colorado at Boulder, Boulder, CO, USA, in 1991. He was an Associate Professor with the Iran University of Science and Technology, Tehran, Iran, from 1993 to 2003, and a Professor with Curtin University, Perth, WA, Australia, from 2004 to 2018. He is currently an Associate Professor with the Department of Engineering, Utah Valley University, Orem, UT, USA. He has coauthored *Power Quality in Power Systems and Electrical Machines* (Elsevier, 2008 and 2015) and the *Power Conversion of Renewable Energy Systems* (Springer, 2011 and 2012). He is an Editor of the IEEE TRANSACTIONS ON SMART GRID and the IEEE POWER ENGINEERING LETTERS.

Airlie Chapman (Member, IEEE) received the B.S. degree in aeronautical engineering and the M.S. degree in engineering research from the University of Sydney, Australia, in 2006 and 2008, respectively, and the M.S. degree in mathematics and the Ph.D. degree in aeronautics and astronautics from the University of Washington, Seattle, in 2013. She is currently a Senior Lecturer with the Department of Mechanical Engineering, University of Melbourne. Her research interests are multiagent dynamics, networked dynamic systems, data-driven control and graph theory with applications to robotics, and aerospace systems.

Stefan Lachowicz (Senior Member, IEEE) received the M.Eng.Sc. and Ph.D. degrees in electronic engineering from the Lodz University of Technology, Lodz, Poland, in 1981 and 1986, respectively, where he was a Research Assistant and an Assistant Professor with the Institute of Electronics from 1994 to 1992. Since 1993, he has been a Lecturer and a Senior Lecturer with the School of Engineering, Edith Cowan University, Joondalup, WA, Australia, since 2001. He has authored and coauthored about 110 research articles. His current research interests include modern power systems, smart energy systems, electric vehicles, and power electronics.